A Novel Octagonal Wound Core for Distribution Transformers Validated by Electromagnetic Field Analysis and Comparison With Conventional Wound Core

Iván Hernández[1,2], Juan C. Olivares-Galván[3], Pavlos S. Georgilakis[4], and José M. Cañedo[2]

[1]Department of Electrical and Computer Engineering, Power Electric System Polytechnic Institute of NYU, Brooklyn, NY 11201 USA
[2]Departamento de Sistemas Eléctricos de Potencia, CINVESTAV Unidad Guadalajara, Zapopan, JAL 45015, Mexico
[3]Departamento de Energía, Universidad Autónoma Metropolitana-Azcapotzalco, Ciudad de México, D.F. 02200, Mexico
[4]School of Electrical and Computer Engineering, National Technical University of Athens, GR 15780 Athens, Greece

This paper analyzes a novel configuration of transformer core, called octagonal wound core (OWC), and shows the minimization of the excitation current and the reduction of the eddy-current losses. The OWC is compared with the conventional wound core (CWC) configuration. The comparison is based on two-dimensional and three-dimensional finite-element method (FEM) simulations, taking into account the nonlinear properties of the magnetic material of the core. The results show that the OWC reduces the excitation current and the eddy-current losses when compared with CWC. Moreover, several combinations of grades of the grain-oriented silicon steel (GOSS) were investigated so as to further reduce the eddy-current losses and the excitation current.

***Index Terms*—Eddy currents, electromagnetic field, finite-element methods, laminations, octagonal wound cores, rolling direction, transformer core, wound core.**

I. Introduction

CONVENTIONAL WOUND CORE (CWC) emerged with the necessity of reducing the size and weight of the distribution transformer, which leads to cost minimization. Other important advantages of CWC are [1]–[3]:

a) Improved distribution of the magnetic flux density in comparison with the stacked core, since the rolling direction is not cut with air gaps in the corners. Wound cores are made of continuous strips so the complete path of the rolling direction is usable and the magnetic flux saturation is reduced.
b) Because of the uniformity of the magnetic flux density along the lamination and the minimization of weight, the eddy-current losses and excitation current are also reduced.
c) Improved performance and increased efficiency.
d) A manufacturer who builds large quantities of identical designs will benefit from the automated processing of CWC.

In the mid-1990s, engineers at AEM developed an innovative core design, called octagonal wound core (OWC). The OWC emerged from CWC with the purpose of reducing cost of manufacturing while preserving all the advantages of the CWC [4]. This paper analyzes this OWC and shows that it helps to reduce the size and the weight of core, the excitation current, and the eddy-current losses.

Manuscript received August 19, 2009; revised November 17, 2009; accepted January 02, 2010. First published March 08, 2010; current version published April 21, 2010. Corresponding author: I. Hernandez (e-mail: ihernand@gdl.cinvestav.mx).

Color versions of one or more of the figures in this paper are available online at http://ieeexplore.ieee.org.

Digital Object Identifier 10.1109/TMAG.2010.2040623

The manufacturing process of the CWC consists of wounding the laminations in one circular mandrel, during this process the laminations are cut and the air gaps are formed. This process damages the characteristics of the cores and their properties are restored through a process of annealing at a temperature between 780–820°C inside of an environment that protects the material (nitrogen mixed with hydrogen). Readers are referred to [5] for more details about annealing process of CWC.

The manufacturing process of the OWC is as follows. Each lamination is cut according to the required length and then every lamination is bent at each of the four corners. Then, the most internal laminations are arranged first and the most external laminations at the end. Only in case that very low no-load loss is required, the OWC is annealed using the same annealing process as in the case of CWC [6].

The process of bending every lamination to achieve the octagonal shape is laborious, but OWC process eliminates the core pressing process in order to form the core rectangular window and OWC in some cases eliminates the core annealing process. The technology of OWC, called *Unicore* technology [4], is very flexible, highly accurate, repeatable, and reliable. Unlike the production of CWC, Unicore does not require any fixed tools, such as mandrels. Unicore laminations are fully formed by the Unicore machine. Authors know that more than 120 Unicore machines have been manufactured until 2008 and Unicores are now being produced or used in many countries. Besides, according to the knowledge of the authors, the OWC permits the mixing of laminations of different grade; with CWC is difficult to mix laminations of different grade (M4 and M5, for example). Authors have visited some transformer manufacturers in Mexico; these manufacturers usually have two Unicore machines, and when one of the machines presents a failure, they continue the manufacturing of cores with the other Unicore machine.

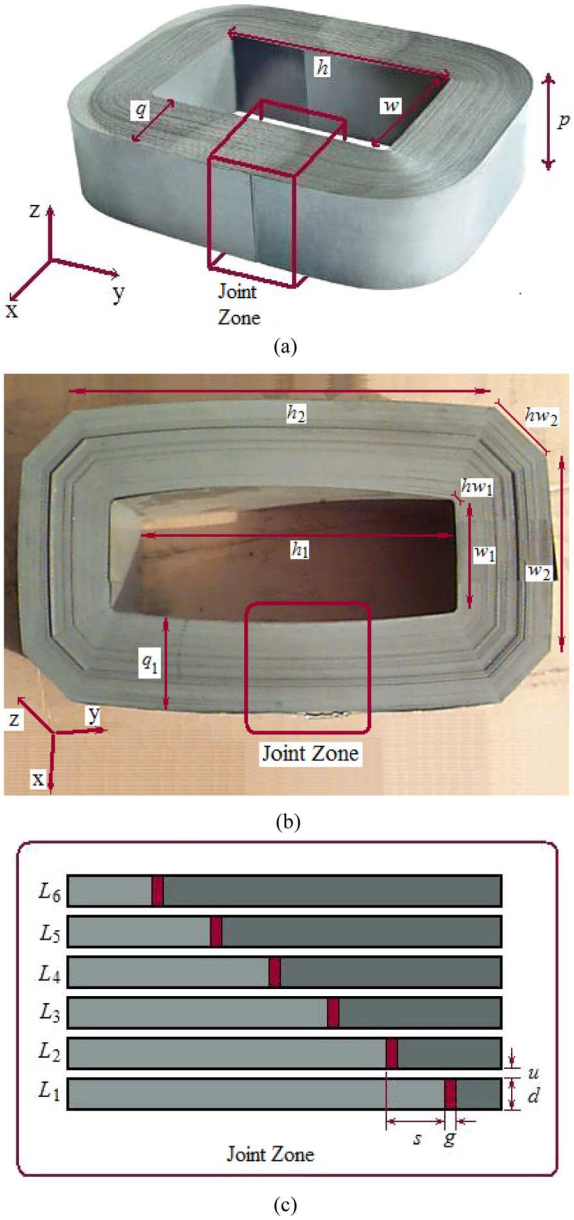

Fig. 1. (a) CWC geometry with its design parameters. (b) OWC geometry with its design parameters. (c) Joint zone in both cores.

The geometry and the design parameters of CWC are shown in Fig. 1(a), where the window height is h, the window width is w, the lamination width is p, and the core width is q. The OWC geometry and design parameters are shown in Fig. 1(b), where the exterior frame height is h_2, the interior frame height is h_1, the exterior frame width is w_2, the interior frame width is w_1, the exterior corner length is hw_2, the interior corner length is hw_1, the core width is q_1, and the lamination width is p. Fig. 1(c) shows the joint zone parameters, i.e., overlap length s, air gap length g, lamination thickness d, and interlamination space u. Appendix A presents the values of core design parameters used in this paper and Appendix B presents the calculations of core weight and core mean length.

Numerical techniques, especially FEM, have been proven very efficient in solving transformer analysis and design problems [1], [7]–[12]. This paper validates the OWC by performing a rigorous electromagnetic comparison between OWC and CWC, launching with details the magnetic flux distribution, excitation current, and eddy-current losses. The numerical results were obtained from two-dimensional and three-dimensional FEM simulations that have taken into account the saturation and the magnetic anisotropy of the core.

II. Electromagnetic Analysis and Simulations

An electromagnetic analysis with FEM was realized with the goal to determinate the magnetic flux distribution and compute eddy-current losses in CWC and OWC. The studies were made using two and three-dimensional simulations, taking into account the saturation and anisotropy, and several grade of grain oriented silicon steel (GOSS), i.e., M4 (0.28 mm), M5 (0.30 mm), M6 (0.35 mm), and a super GOSS M5H2 (0.30 mm).

The magnetic flux density distribution and eddy-current losses were determined by the solution of the vector potential formulation $\mathbf{A}$ in the frequency domain [13], [14]:

$$j\omega\sigma\mathbf{A} + \nabla \times \left(\frac{1}{\mu}\nabla \times \mathbf{A}\right) = 0 \tag{1}$$

where μ represents a tensor of the permeability of the different GOSS used and σ is its conductivity. For the magnetic anisotropy, the permeability in the rolling direction plane varies in accordance with the saturation curves shown in Appendix C, while for the perpendicular direction to the rolling plane a relative permeability three times lower than the relative permeability of the rolling direction is considered, e.g., $\mu_r = (1/3) * 25\ 000$ for the M5 GOSS [18]. The nonlinear characteristics of the GOSS laminations in the frame of the time harmonic analysis produce often high computational cost; the technique adopted to reduce the computational cost was established in [15], where authors consider an effective B–H curve based on the energy equivalence for a time period cycle T.

In case of conductivity, the manufacturer specifies only a volume resistivity (48×10^{-6} ohm-cm at 20°C); therefore this value was considered to be isotropic.

The distribution of the dissipated power can be calculated from [16]:

$$P = \frac{1}{2}\mathrm{Re}\left[\sum_{i=1}^{n}(\rho_i Je_i^* \cdot Je_i)V_i\right] \tag{2}$$

where n represents the number of elements, ρ_i is a diagonal tensor of resistivity of the GOSS, Je_i is the eddy-current density vector of the element i, and V_i is the volume of the element i. Eddy-current density is given by

$$Je_i = -j\sigma\omega\mathbf{A}_i = -\sigma\frac{1}{n}\sum_{i=n}^{n}\mathbf{N}_A^T\mathbf{A}_i \tag{3}$$

where $\mathbf{N}_\mathrm{A}$ represents the element shape functions for the vector potential $\mathbf{A}$.

Commercial finite-element software [14] was used to perform the simulations shown in this paper. In particular, 2-D FEM models were used to simulate every lamination on the core

width. Three-dimensional FEM models were used to verify that the perpendicular component of the magnetic flux density on the rolling direction is negligible by simulating only groups of maximum 12 laminations due to the computational memory consumed. Moreover, 3-D FEM models were used to validate the accuracy of the 2-D FEM models. In particular, in the 3-D FEM model, we used about 423 800 tetrahedral elements producing approximately 212 466 nodes. It is also important to mention that for the mesh volume we used the technique of extruding the meshed area and special care is taken in the laminations element size to be fine, i.e., the maximum sides size must not exceed the thickness of laminations, so as to capture the skin depth and obtain accurate calculation of the losses and excitation current. An important parameter in eddy-current calculation is the skin depth δ:

$$\delta = \sqrt{\frac{1}{\pi f \mu \sigma}}. \tag{4}$$

The skin depth considered was function of the total width of the number of laminations used [17].

The boundary conditions are on tanks walls on which magnetic insulation is set.

The excitation current is determined as follows: from the magnetic flux density value obtained in each lamination we obtained for each lamination the exciting power (volt-ampere per kilogram), VA_k, using the GOSS manufacturer curves [18]. The total exciting power was obtained by the sum of the exciting power of each lamination; therefore the exciting current percentage is given by

$$\%I_{\mathrm{exc}} = (100)\frac{\sum_{k=1}^{k=nl} \mathrm{VA}_k}{\mathrm{VA}_{\mathrm{rate}}} \tag{5}$$

where VA_k is the exciting power in each lamination, nl is the number of laminations, and $\mathrm{VA}_{\mathrm{rate}}$ is the transformer rating (volt-ampere).

III. Results and Discussion

A. Distribution of the Magnetic Flux Density

The magnetic flux density B in CWC is shown in Fig. 2. For this simulation we used GOSS M5 (0.30 mm). We excite the core to reach an average $B = 1.70$ T in the core cross section. This value is our reference value that permitted the comparison and verification with the eddy losses calculated with the values specified by the GOSS manufacturer; for example in the M5 case for $\mathrm{B} = 1.70$ T the maximum core loss specified by the manufacturer is about 1.83 W/kg, but only about 73% of this value could be considered eddy losses [18]. Fig. 2(a) shows that the magnetic flux density is smaller and useless in the corners of the CWC, and from this conclusion, it is possible to trim the CWC, thereby reducing the cost of manufacturing and improving the transformer efficiency through innovate core design OWC [4]. Fig. 2(b) shows the magnetic flux lines distribution in a CWC and Fig. 2(c) illustrates the magnetic flux distribution in its joint zone, where the magnetic flux distortion is evident. This

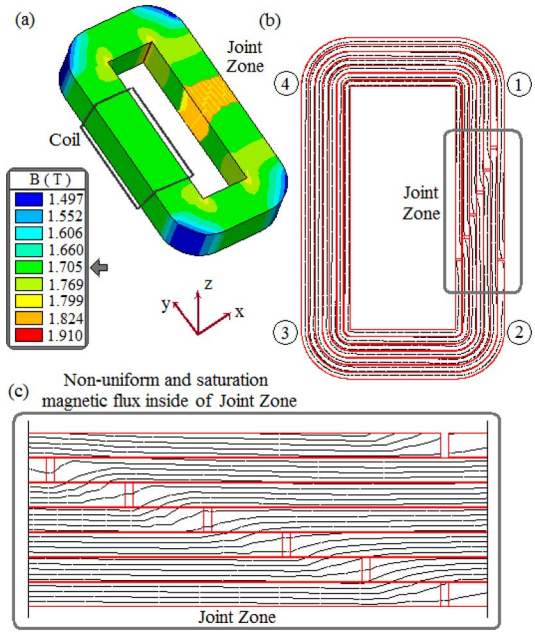

Fig. 2. (a) Magnetic flux density distribution in a CWC. (b) Magnetic flux lines distribution in a CWC. (c) Nonuniform and saturation magnetic flux inside of Joint Zone.

magnetic flux distribution on the CWC was compared with the results obtained for the OWC, using the same GOSS (M5), and the same excitation. Fig. 3(a) shows the magnetic flux density in an OWC. It is evident that the magnetic flux density increases with respect to the CWC values [see Figs. 2(a) and 3(a)]. The same excitation current produces a $B = 1.710$ T in the OWC, and $B = 1.705$ T in the CWC. This means that an OWC is able to reach greater magnetic flux density than the CWC using the same excitation current. Therefore, it is possible to get a reduction in the excitation current of OWC to obtain the same magnetic flux density. This reduction in the excitation current is because the core length in an OWC is smaller than in the CWC and this causes a reduction of core reluctance.

However, there is an inconvenience in the OWC with respect to the CWC: there is a bigger zone in the OWC in the interior frame corner where the magnetic flux density raises to saturation values (in this example $B = 1.908$ T). Figs. 2(c) and 3(c) show that there is no significant difference between the magnetic flux in the joint zone of both CWC and OWC configurations. We compared also the magnetic flux density along the lamination. For this we made a path along the lamination in the middle of one random lamination. We denoted the rolling direction change by the consecutive numbers 1 to 4 clearly specified in Figs. 2(b) and 3(b). The transformer coils are in the opposite leg to the joint zone.

Figs. 4(a) and (b) show the magnetic flux density component B_x and B_y, respectively, along the lamination, and Fig. 4(c) presents the norm of the magnetic flux density. The B_z was also determined, however, it was found that its magnitude was negligible in comparison with B_x and B_y components, which is reasonable since B_z component is perpendicular to the rolling plane. It can be observed from Figs. 4(a) and (b) that B_x and B_y components have only a small difference on magnitude for

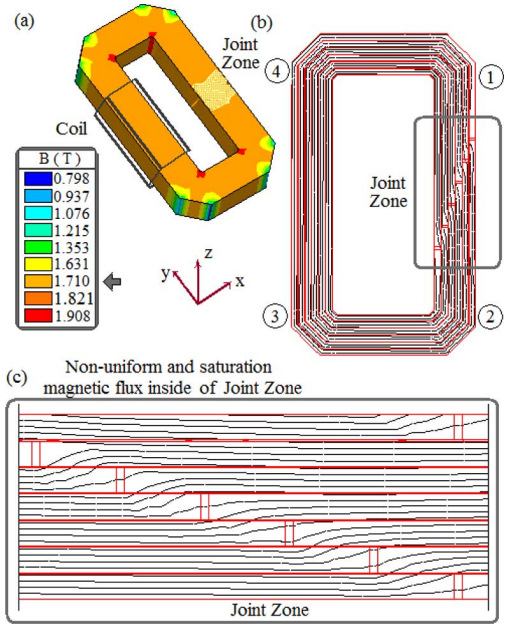

Fig. 3. (a) Magnetic flux density distribution in an OWC. (b) Magnetic flux lines distribution in an OWC. (c) Nonuniform and saturation magnetic flux inside of Joint Zone.

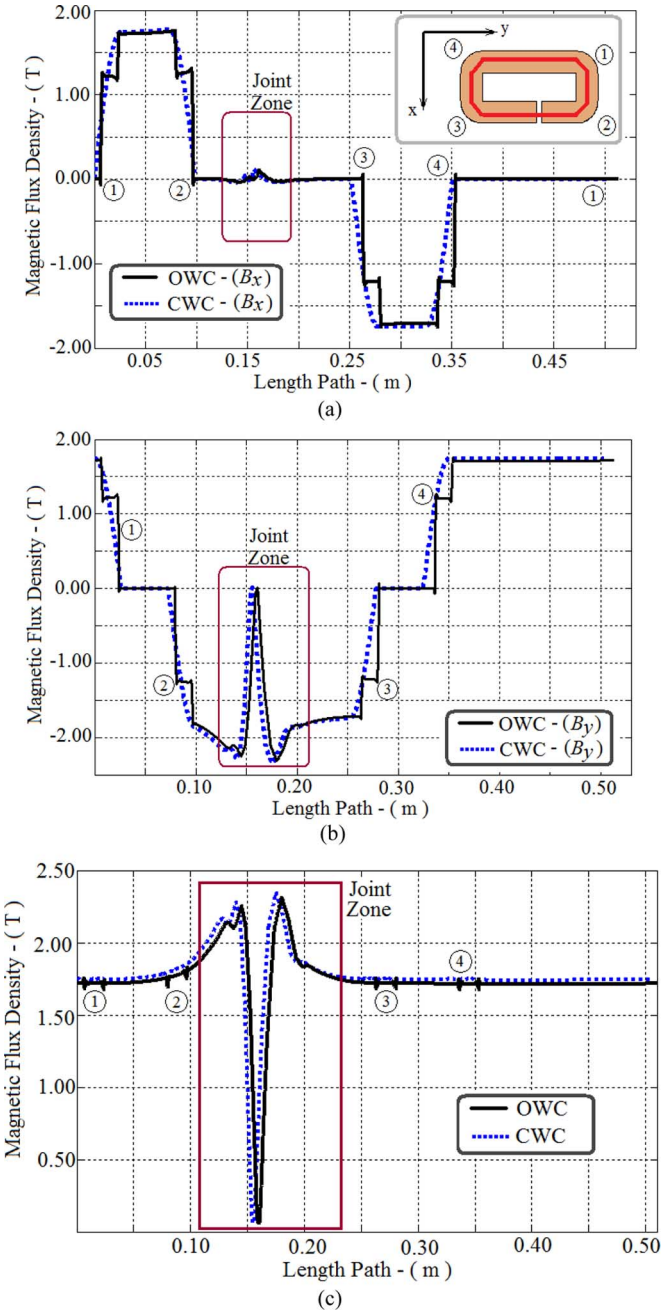

Fig. 4. (a) Magnetic flux density component B_x along the lamination, points 1 to 4 indicate change in the rolling direction. (b) Magnetic flux density component B_y. (c) Magnetic flux density norm components along the lamination.

CWC and OWC. Moreover, in the OWC the magnetic flux density presents a square shape, due to its geometry itself. The magnetic flux density norm from the three components (B_x, B_y, and B_z) was determined and it is shown in Fig. 4(c); it can be seen that the magnetic flux is uniform along the lamination except in its joint zone.

There is a magnetic flux drop in the cross-section area of the core leg, which means that the internal laminations have greater magnetic flux density values than the external laminations. This decrease on the slope in both core configurations was analyzed and compared. For this, we realized a cut in the opposite leg of the joint zone, shown in Fig. 5(a). The core is excited to reach a desired magnetic flux density $B = 1.70$ T in the cross-section area of the core leg. Fig. 5(b) shows the slopes in both cores using the same excitation current. It can be noticed that the magnetic flux density slope for OWC, m_O, is greater than the CWC slope, m_W. More specifically, $m_O \approx 1.16 \cdot m_W$. This greater slope produces a reduction in the B values at the external laminations and consequently a reduction in eddy-current losses for the OWC.

We simulated and compared the magnetic flux density distribution and its slopes in both cores for different grades and thicknesses of GOSS. The obtained results are shown in Fig. 6 for the cases of M4, M5, M6, and M5H2 grades of magnetic material.

B. Eddy-Current Losses and Excitation Current Comparison in CWC and OWC

According to Fig. 6, OWC has a greater magnetic flux density slope for the different grades and thicknesses of GOSS analyzed. Table I shows the relation of the magnetic flux density slope values with the eddy-current losses (Peddy) and excitation current (Iexc) in both core configurations. These values were obtained when the cross-section area in the core leg reaches a magnetic flux density of 1.70 T. Table I also shows that the eddy-current losses in OWC were decreased by up to 17.68% in comparison with CWC (for the case of M6 electrical steel).

It can be also seen from Table I that using an OWC it is possible to simultaneously reduce the eddy-current losses and the excitation current. Using M5H2 electrical steel, it is possible to reduce the excitation current by 1.12% when using OWC instead of CWC.

If besides the OWC, a super GOSS is used (M5H2), then the eddy-current losses will be decreased by about 25% in comparison with M5, as Table I shows. The M4 electrical steel also pro-

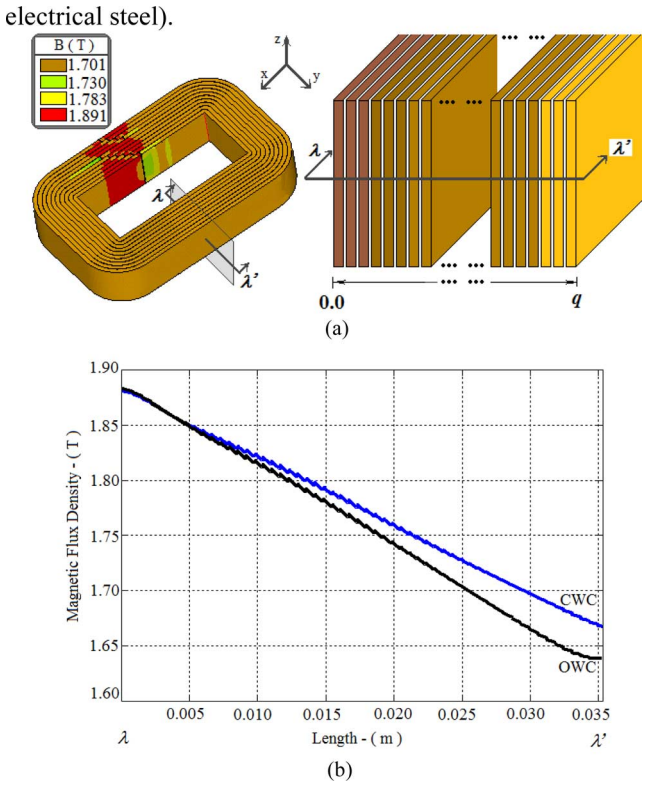

Fig. 5. (a) Cross-section area in which the drop of the magnetic flux density slope is analyzed. (b) Drop of the magnetic flux density slope on both core configurations.

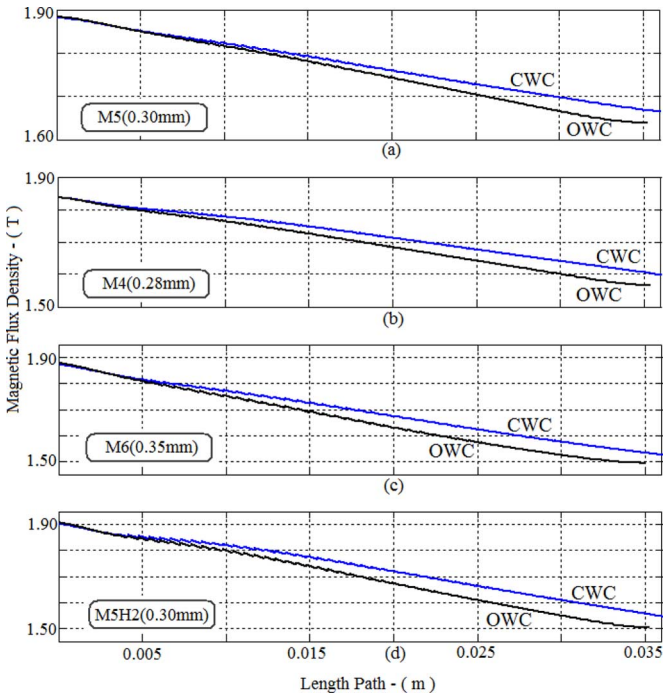

Fig. 6. Magnetic flux density slopes comparison. (a) M5 electrical steel slope. (b) M4 electrical steel slope. (c) M6 electrical steel slope. d) M5-H2 electrical steel slope.

vides important decrease in eddy-current losses compared with the M5.

TABLE I
COMPARISON OF MAGNETIC FLUX DENSITY SLOPES, EXCITATION CURRENT, AND EDDY-CURRENT LOSSES IN CWC AND OWC

Type	*GOSS*	*Slope*	*%Δ Slope*	*Iexc*	*% Δ Iexc*	*Peddy*	*% Δ Peddy*
CWC	M4	6.4948		0.9025		0.8694	
OWC	M4	7.5572	16.35	0.8941	0.93	0.7209	17.08
CWC	M5	5.7528		1.0000		1.0000	
OWC	M5	6.8453	18.99	0.9865	1.35	0.8318	16.82
CWC	M6	8.9736		1.1210		1.3717	
OWC	M6	10.7342	19.61	1.1106	0.92	1.1291	17.68
CWC	M5H2	9.7269		0.8158		0.8781	
OWC	M5H2	11.2982	16.15	0.8066	1.12	0.7319	16.64

All the values are given in per unit (pu). The reference values are the excitation current and the eddy-current losses for M5 electrical steel.

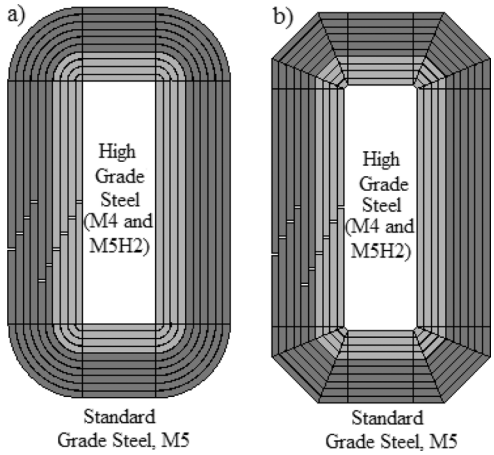

Fig. 7. Mixing grade electrical steel, high grade steel in the internal laminations and standard grade in external laminations. (a) CWC, (b) OWC.

Regarding the excitation current, Table I shows that the OWC decreases the excitation current by up to 1.35%. Use of M6 instead of M5 increases the excitation current by about 11%, which means that M6 has higher value of volt ampere/kg. On the other hand, use of M5H2 for core construction decreases the excitation current by up to 18% for CWC and almost 20% for OWC. With these results it is evident that the manufacturing of OWC is favorable to reduce the excitation current and the eddy-current losses.

C. Mixing of Electrical Steel of Different Grade in the Cores

With the goal to further reduce the excitation current and the eddy-current losses, we investigated the mixing technique of grade in the core laminations [6]. The simulation consisted of combining the high GOSS analyzed in this work, M4 and M5H2, with the standard grain oriented M5. High-grade steel was placed in the internal frame laminations where the magnetic flux density is greater, and the standard grade steel was placed in the external frame laminations, as Fig. 7 shows. We carried out a mixing of the electrical steel of different grade ranging from 0% to 50% of the total lamination in the core. The results are shown in Tables II and III and in graphical form in Figs. 8 and 9.

Analyzing Tables II and III and Figs. 8 and 9, the following conclusions are drawn:

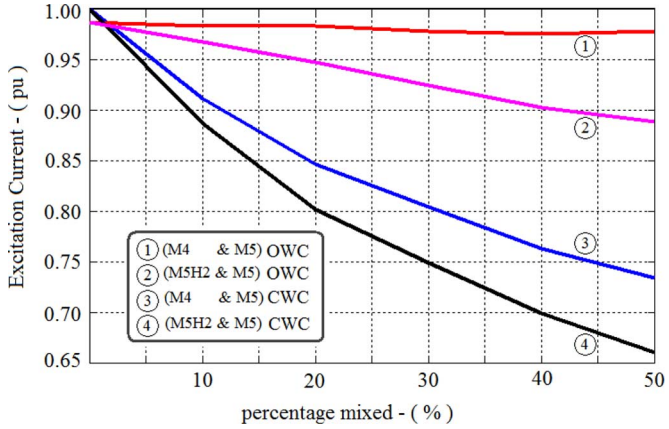

Fig. 8. Excitation current as a function of the percentage of grade steel mixed, given in Tables II and III. Curves 1 and 2 show the results for an OWC, while curves 3 and 4 present the results for a CWC. The reference values are the excitation current for M5 electrical steel.

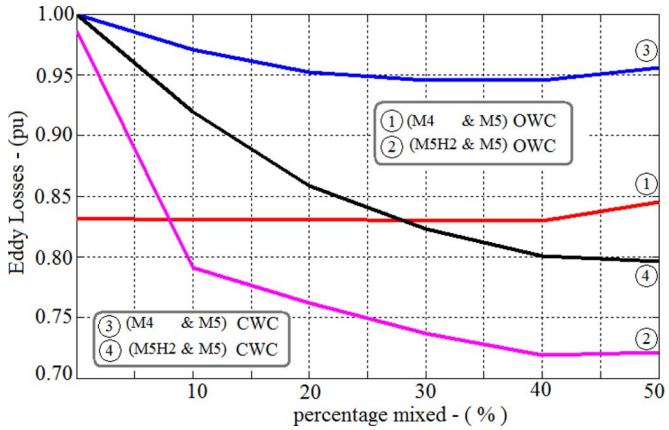

Fig. 9. Eddy-current losses as a function of the percentage of grade steel mixed, given in Tables II and III. Curves 1 and 2 show the results for an octagonal core, while curves 3 and 4 present the results for a wound core. The reference values are the eddy-current losses for M5 electrical steel.

TABLE II
COMPARISON OF EXCITATION CURRENT AND EDDY-CURRENT LOSSES IN CWC AND OWC FOR MIXING M4 & M5

Mixing GOSS	*Iexc CWC*	*Iexc OWC*	*Peddy CWC*	*Peddy OWC*
0 % M4 -100% M5	1.0000	0.9865	1.0000	0.8318
10 % M4 - 90% M5	0.9108	0.9832	0.9705	0.8304
20 % M4 - 80% M5	0.8461	0.9832	0.9524	0.8307
30 % M4 - 70% M5	0.8048	0.9776	0.9453	0.8294
40 % M4 - 60% M5	0.7636	0.9751	0.9453	0.8299
50 % M4 - 50% M5	0.7348	0.9776	0.9559	0.8452

1) The excitation current is decreased in both cores with the increase of the percentage mixed of different grades of GOSS.
2) The mixing technique of different grades of GOSS is more beneficial for a CWC than for an OWC, in order to reduce the excitation current (curves 3 and 4 of Fig. 8).
3) The mixing of M4 and M5 in an OWC has a minimum effect in order to reduce the eddy-currents (curve 1 of Figs. 8 and 9).
4) The eddy-current losses are decreased in both cores with the increase of the percentage mixed of different grades of GOSS, except for the case when the percentage mixed exceeds the 40%–60% in an OWC.
5) The best mixing to decrease the excitation current is the relation 50% M5H2–50% M5 in a CWC, which provides a reduction of about 33%.
6) The best mixing to decrease the eddy-current losses is the relation 40% M5 H2–60% M5 in an OWC, which provides a reduction of about 28%.

TABLE III
COMPARISON OF EXCITATION CURRENT AND EDDY-CURRENT LOSSES IN CWC AND OWC FOR MIXING M5H2 AND M5

Mixing GOSS	*Iexc CWC*	*Iexc OWC*	*Peddy CWC*	*Peddy OWC*
0 % M5H2-100% M5	1.0000	0.9865	1.0000	0.9865
10 % M5H2 - 90% M5	0.8869	0.9669	0.9194	0.7908
20 % M5H2 - 80% M5	0.8021	0.9471	0.8584	0.7623
30 % M5H2 - 70% M5	0.7492	0.9245	0.8232	0.7364
40 % M5H2 - 60% M5	0.6997	0.9027	0.8005	0.7186
50 % M5H2 - 50% M5	0.6613	0.8883	0.7958	0.7213

All the values are given in per unit. The reference values are the excitation current and the eddy current losses for M5 electrical steel. It was about 128.8675 W/m

IV. CONCLUSION

This paper investigates the OWC with the aim to reduce the excitation current and the eddy-current losses. The analysis and simulation results introduced in this paper show the advantages of the OWC in comparison with the CWC in terms of reduced excitation current and eddy-current losses. Moreover, this paper investigates the mixing of GOSS of different grades in OWC, which mixing can be much easier implemented for the OWC than the CWC technology.

The results show that the OWC decreases the eddy-current losses by about 16% and the excitation current by 1.3%. It has been also found that the GOSS mixing technique in the CWC is more beneficial to decrease eddy-current losses and excitation current than in the OWC. The mixing of high grades of GOSS in the internal laminations with standard grades of GOSS reduces considerably the eddy-current losses. The reduction of eddy-current losses and excitation current depends on the percentage of GOSS steel mixed. The research work and the results presented in this paper are very useful for the design and manufacturing of transformer cores.

APPENDIX A
VALUES OF CORE DESIGN PARAMETERS

Table IV Shows the Values of the 16 Core Design Parameters.

APPENDIX B
CALCULATION OF WEIGHT AND MEAN LENGTH OF WOUND CORES

The following equations are used to determine the core weight and the core mean length for the analyzed core configurations. These equations have been verified with computer aided design (CAD) software as well as with measurements.

TABLE IV
VALUES OF THE DESIGN PARAMETERS

#	*Parameter*	*Value*	#	*Parameter*	*Value*
1	h	153.00	9	h_1	153.00
2	w	42.86	10	h_2	183.00
3	p	36.00	11	w_l	46.50
4	q	37.82	12	w_2	71.10
5	s	10.00	13	hw_1	2.60
6	g	1.00	14	hw_2	31.00
7	d	0.30	15	p	36.00
8	u	0.015	16	q_1	36.00

All the values are given in mm. Parameter d is the lamination thickness and it has the following values for the following grades: M5 (0.30mm), M4 (0.28mm), M6 (0.35mm) and M5H2 (0.30mm).

A. CWC

The surface occupied [in Fig. 7(a)] by the laminations is given by

$$A_{c(\mathrm{CWC})} = fs \cdot q[2(h+w)+\pi \cdot q] \tag{1B}$$

where the frame height is h, the frame width is w, the lamination width is p, the core width is q, and the stacking factor is fs. Consequently, the core volume is given by

$$V_{c(\mathrm{CWC})} = fs \cdot p \cdot q[2(h+w)+\pi \cdot q]. \tag{2B}$$

Using the specific weight density for the GOSS, ρ_e, the core weight is computed as follows:

$$P_{c(\mathrm{CWC})} = fs \cdot \rho_e \cdot p \cdot q[2(h+w)+\pi \cdot q]. \tag{3B}$$

The mean core length for a CWC is given by

$$\ell_{m(\mathrm{CWC})} = 2(h+w)+\pi \cdot q. \tag{4B}$$

B. OWC

The surface occupied [in Fig. 7(b)] by the core width in an OWC is given by

$$A_{c(\mathrm{OWC})} = fs \cdot q_1[h_1+h_2+w_1+w_2+2(hw_1+hw_2)]. \tag{5B}$$

The core volume is

$$V_{c(\mathrm{OWC})} = fs \cdot p \cdot q_1[h_1+h_2+w_1+w_2+2(hw_1+hw_2)]. \tag{6B}$$

The core weight is

$$P_{c(\mathrm{OWC})} = fs \cdot \rho_e \cdot p \cdot q_1[h_1+h_2+w_1+w_2+2(hw_1+hw_2)]. \tag{7B}$$

The core mean length for an OWC is given by

$$\ell_{m(\mathrm{OWC})} = 2(h+w+4 \cdot q_1 \cdot \sin\theta). \tag{8B}$$

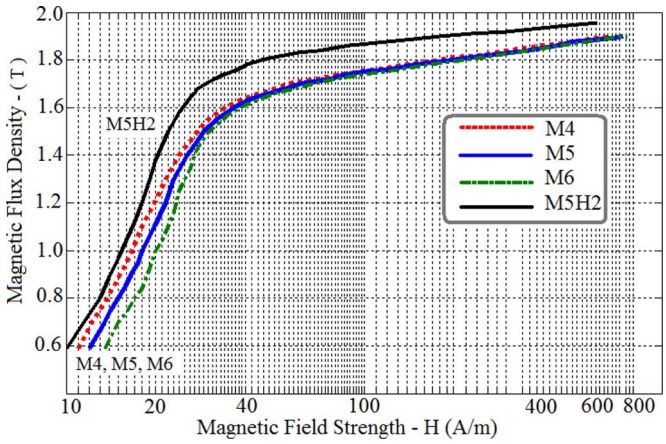

Fig. 10. B–H curves for the GOSS lamination applied.

The following relation holds between the width of the CWC and the width of the OWC:

$$q = q_1 + 0.5 \cdot hw_1 \cdot \sec\theta \tag{9B}$$

where θ is the angle for the OWC construction corner; for this work we used $\theta = \pi/8$.

The above formulations of area and volume present about $+2\%$ error in comparison with calculations based on CAD software.

Approximately 6% reduction on the volume of OWC was found in comparison to the volume of the CWC; this reduction depends on the manufacturer building factors.

APPENDIX C

Fig. 10 shows B–H curves for the GOSS lamination applied.

REFERENCES

[1] P. S. Georgilakis, *Spotlight on Modern Transformer Design*. London, U.K.: Springer, 2009.
[2] J. H. Harlow, *Electric Power Transformer Engineering*. Boca Raton, FL: CRC, 2004.
[3] *CRGO Wound Cores Products Information*, Vardhman Stampings pvt. Ltd. [Online]. Available: http://www.vardhmanstampings.com/product_crgo_wounds.thm
[4] *Aem Unicore-Innovation in Transformer Cores and Manufacturing Data Catalog*. Gillman, Australia: Aem cores PTY, LTD., Oct. 2008.
[5] P. S. Georgilakis, N. D. Hatziargyriou, N. D. Doulamis, A. D. Doulamis, and S. D. Kollias, "Prediction of iron losses of wound core distribution transformers based on artificial neural networks," *Neurocomputing*, vol. 23, no. 1–3, pp. 15–29, Dec. 1998.
[6] T. D. Kefalas, P. S. Georgilakis, A. G. Kladas, A. T. Souflaris, and D. G. Paparigas, "Multiple grade lamination wound core: A novel technique for transformer iron loss minimization using simulated annealing with restarts and an anisotropy model," *IEEE Trans. Magn.*, vol. 44, no. 6, pp. 1082–1085, Jun. 2008.
[7] M. Breschi and A. Cristofolini, "Experimental and numerical analysis of stray field from transformers," *IEEE Trans. Magn.*, vol. 43, no. 11, pp. 3984–3990, Nov. 2007.
[8] E. I. Amoiralis, M. A. Tsili, P. S. Georgilakis, A. G. Kladas, and A. T. Souflaris, "A parallel mixed integer programming-finite element method technique for global design optimization of power transformers," *IEEE Trans. Magn.*, vol. 44, no. 6, pp. 1022–1025, Jun. 2008.

[9] S. L. Ho, Y. Li, R. Y. Tang, K. W. E. Cheng, and S. Y. Yang, "Calculation of eddy current field in the ascending flange for the bushings and tank wall of a large power transformer," *IEEE Trans. Magn.*, vol. 44, no. 6, pp. 1522–1525, Jun. 2008.
[10] G. Štumberger, S. Seme, B. Štumberger, B. Polajžer, and D. Dolinar, "Determining magnetically nonlinear characteristics of transformers and iron core inductors by differential evolution," *IEEE Trans. Magn.*, vol. 44, no. 6, pp. 1570–1573, Jun. 2008.
[11] J. V. Leite, A. Benabou, N. Sadowski, and M. V. F. da Luz, "Finite element three-phase transformer modeling taking into account a vector hysteresis model," *IEEE Trans. Magn.*, vol. 45, no. 3, pp. 1716–1719, Mar. 2009.
[12] E. I. Amoiralis, P. S. Georgilakis, M. A. Tsili, and A. G. Kladas, "Global transformer optimization method using evolutionary design and numerical field computation," *IEEE Trans. Magn.*, vol. 45, no. 3, pp. 1720–1723, Mar. 2009.
[13] O. Biro, K. Preis, and K. R. Richter, "Various FEM formulations for the calculation of transient 3D eddy currents in nonlinear media," *IEEE Trans. Magn.*, vol. 31, no. 3, pp. 1307–1312, May 1995.
[14] *ANSYS Reference Manual*, 8th ed. Canonsburg, PA: SAS IP INC., 2003.
[15] N. A. Demerdash and D. H. Gillott, "A new approach for determination of eddy currents and flux penetration in nonlinear ferromagnetic materials," *IEEE Trans. Magn.*, vol. MAG-10, no. 3, pp. 682–685, 1974.
[16] J. Xu, A. Lakhsasi, Z. Yao, and V. Rajagopalan, "A practical modeling method for eddy-current losses computation in laminated magnetic cores," in *Proc. IEEE 31st Industry Applications Soc. Annu. Meet.*, Oct. 1996, vol. 3, pp. 1532–1537.
[17] A. Bermudez, D. Gomez, and P. Salgado, "Eddy-current losses in laminated cores and the computation of an equivalent conductivity," *IEEE Trans. Magn.*, vol. 44, no. 12, pp. 4730–4738, Dec. 2008.
[18] *Armco Oriented and Tran-Cor H Electrical Steels Data Catalog*. Middletown, Ohio: Armco Steels Inc., 1979.

Iván Hernández (S'06) was born in Salamanca, Guanajuato, México, in 1979. He received the B.Sc. degree in electrical engineering from the University of Guanajuato, Mexico, in 2002, and the M.Sc. degree in electrical engineering from the CINVESTAV Guadalajara, México, in 2005. He is a Ph.D. student at CINVESTAV Guadalajara and currently a visitor at Polytechnic Institute of New York University.

He was an electrical engineer designer for two years in FMS Ingeniería, Guadalajara, México. His research interests are the numerical analysis applied to electrical machine design, and software simulation tools particularly for electromagnetic fields.

Juan Carlos Olivares-Galván (M'04) was born in Michoacán, México, in 1969. He received the B.Sc. and M.Sc. degrees in electrical engineering from Instituto Tecnológico de Morelia, Mexico, in 1993 and 1997, respectively, and the Ph.D. degree in electrical engineering from CINVESTAV, Guadalajara, México, in 2003.

He is currently a Professor at the Departamento de Energía of Universidad Autónoma Metropolitana (UAM). He was with Electromanufacturas S.A. de C.V., where he was a transformer design engineer for eight years. He was a Visiting Scholar at Virginia Tech, Blacksburg, in 2001. His main interests are related to the experimental and numerical analysis of transformers.

Pavlos S. Georgilakis (M'01) was born in Chania, Greece, in 1967. He received the Diploma in electrical and computer engineering and the Ph.D. degree from the National Technical University of Athens (NTUA), Athens, Greece, in 1990 and 2000, respectively.

He is currently a Lecturer at the School of Electrical and Computer Engineering of NTUA. From 2004 to 2009, he was an Assistant Professor in the Production Engineering and Management Department of the Technical University of Crete, Greece. From 1994 to 2003, he was with Schneider Electric AE, where he worked in the transformer industry as transformer design engineer for four years, and research and development manager for three years. He is the author of the book *Spotlight on Modern Transformer Design* (Springer, 2009). His current research interests include transformer design and power systems optimization.

Jose Manuel Cañedo (M'96) was born in Mazatlan, Sinaloa, Mexico, in 1950. He received the B.Sc. degree from the University of Guadalajara in 1971, the M.Sc. degree in electrical engineering from the National Polytechnic Institute (IPN) of Mexico in 1980, and the Ph.D. degree from the Moscow Power Institute, URSS, in 1985.

From 1988 to 1994, he was a researcher at CFE Mexico. From 1994 to 1997, he was at the University of Guadalajara and since 1997, he has been with CINVESTAV Guadalajara Campus, Mexico, as a Professor in the graduate programs in Electrical Engineering. His research interests include nonlinear robust control of power systems, electric machines, and electromagnetic fields.